Effect of hysteresis on the critical state behavior of an unsaturated silty soil

A. R. Estabragh[1], M. Moghadas[2], A. A. Javadi[3], M. Babalar[4]

[1] Associate Professor, Faculty of Soil and Water Engineering, University of Tehran, PO BOX 4411 Karaj 31587-77871, Iran

Tel: +98 26 32241119, Fax: +98 26 32226181, Email: raeesi@ut.ac.ir

[2] Senior Expert of Water, Isfahan Regional Water Company, PO BOX 391, Isfahan 76473-81646, Iran

Tel: +98 3136615360 ,Fax: +98 3136627500,Email: Moghadas@esrw.ir

[3]Professor,Computational Geomechanics Group, Department of Engineering, University of Exeter, Devon, EX4 4QF, UK

Tel: +44 1392 723640, Fax: +44 1392 217965, Email: A.A.Javadi@exeter.ac.uk

[4]Research Assistant, Faculty of Soil and Water Engineering, University of Tehran, PO BOX 4411 Karaj 31587-77871, Iran

Tel: +98 26 32241119, Fax: +98 26 32226181, Email: babalar@ut.ac.ir

Corresponding Author**:** A.R. Estabragh

Abstract

In this work the effect of hysteresis on the critical state behavior of unsaturated soils was investigated through conducting a number of controlled suction triaxial tests on samples of an unsaturated silty soil. The slurry method was used for preparing the samples for the main tests. The tests were carried out in a double-walled triaxial cell. In the experiments the samples were consolidated isotropically to virgin state at suctions of 0, 100, 200, 250

and 300 kPa on drying and wetting paths of soil water characteristic curve. Then they were sheared under constant suction at various constant cell pressures. The results of the drained triaxial tests were used to determine the effect of the hysteresis phenomenon on the characteristics of the critical state framework. The obtained data were examined in terms of mean net Bishop's stress (p^*) (by including degree of saturation) or $\bar{p}$ (i.e. the mean total stress in excess of pore air pressure), deviator stress (q), suction (s) and specific volume (v) as state variables. The results show that the critical state lines (CSLs) for the dry and wet paths are not parallel for different suctions in the $q:p^*$ or $q:\bar{p}$ space. The slopes and intercepts of the CSLs in this space are functions of suction. In addition, the critical state lines in the v: Ln p^* or v: Ln $\bar{p}$ plane are not parallel for drying and wetting paths and the slope and intercept of them are also functions of suction. The results also indicated that two frameworks showed similar trend of critical state parameters but the framework based on p^* is more reliable than the one based on the $\bar{p}$.

Key words: unsaturated soil, hysteresis, degree of saturation, soil water characteristic curve, consolidation, shearing, critical state

INTRODUCTION

Background

The role of soil water characteristic curve (SWCC) is important in the description of the behavior of unsaturated soils. The soil water characteristic curve presents the relationship between the soil suction and gravitational water content or volumetric water content or degree of saturation. Hydraulic hysteresis occurs during drying and wetting in soils.

Hydraulic hysteresis results in the relationship between degree of saturation and suction being significantly different depending on whether water is moving into or out of the soil. Hydraulic hysteresis means that two samples of the same soil subjected to the same value of suction can be at significantly different values of degree of saturation if one is on a drying path and the other is on a wetting path (Wheeler et al. 2003). At the same suction, the larger voids of a soil with higher degree of saturation are filled with more water than the voids with lower degree of saturation. Therefore, the soil water characteristic curve is affected by the dependency of S_r (degree of saturation) on e (void ratio).

The constitutive models describing the hydraulic hysteresis behavior of unsaturated soils can be divided into two groups. In the first group the effect of suction on S_r is considered to be more important than the effect of e (Tamagnini, 2004 and Li, 2005). The second group consider the dependency of soil water characteristic curve on e and S_r (Gallipoli et al. 2003; Nuth and Laloui 2008 and Masin 2010). It is generally known that the mechanical behavior of soil on dry and wet paths of SWCC are not the same and they are under the influence of hysteresis (Guan et al. 2010, Khalili and Zargarbashi 2010, Khoury and Miller 2012 and Lu et al. 2013). Estabragh et al. (2017) conducted isotropic consolidation tests on samples of silty soil with initial void ratio of 0.62, water content of 22% and degree of saturation of 93% under constant suction on dry and wet paths of SWCC. They reported that the mechanical behavior of the soil is not the same at the same suction on wetting and drying paths. Sun et al. (2016) studied the effect of suction history on the hydraulic and stress-strain behavior of unsaturated soils through experimental tests. They concluded from the results of the tests that if the maximum suction that a sample has experienced in the past is less than the residual suction, the sample would have higher

shear strength. Rojas et al. (2017) proposed a model for simulation the hydraulic hystersis of soil and effect of volumetric deformation on the soil water characteristic curve. Li and Yang (2018) proposed a hydromechanical constitutive model for unsaturated soil with different overconsolidation ratio. The fundamental framework of this model was degree of saturation and skeleton stress. Tang et al. (2018) present a numerical model for consolidation of unsaturated soil including the effect of hydraulic hysteresis. They showed that the different location of hydraulic states on SWCC results in different settlements and excess pore pressure. Khosravi et al. (2018) conducted a number of tests on samples of an unsaturated soil to determine the relationship between G_{max} with suction. They created desired suction on the drying path of SWCC and then subjected the sample to loading and unloading with the suction kept constant. They found that the variations of G_{max} is dependent on the value of void ratio of the sample

Elasto-pastic constitutive models

In the past few years, important developments in understanding and modelling the behavior of unsaturated soils have been published by many researchers (e.g., Alonso et al. 1990; Wheeler and Sivakumar 1995; Cui and Delage 1996 and Farias et al. 2006). These models are expressed in terms of the mean net stress state $\bar{p}$ (i.e. the mean total stress in excess of pore air pressure) and suction, s (u_a - u_w). These models do not include the degree of saturation, S_r for describing the relative portions of air and water inside the soil voids. Therefore, they are not able to provide correct predictions when the influence of hydraulic hysteresis on the mechanical behavior of soil is important. In other words, the irreversible deformation of soils during drying and wetting is a consequence of the hysteretic variation of degree of saturation that is not included in these models. In order

97 to overcome these limitations, researchers such as Jommi (2000), Vaunat et al. (2000),
98 and Gallipoli et al. (2003) proposed elasto-plastic models that include the
99 hydromechanical coupling. The disadvantages of this type of approach are the difficulty
100 and complexity arising in terms of constitutive equations, the need to couple two separate
101 models and the large numbers of parameters involved. In contrast, Buisson and Wheeler
102 (2000), Vaunat et al. (2000) and Wheeler et al. (2003) proposed a single framework in
103 order to explain both mechanical and water retention behaviors. Of these three models,
104 Buisson and Wheeler (2000) and Wheeler et al. (2003) include coupling in both
105 directions, whereas Vaunat et al. (2000) incorporates only the influence of mechanical
106 behavior on water retention behavior (but not vice versa).
107 Wheeler et al. (2003) proposed a model for mechanical behavior and SWCC where both
108 aspects of soil behavior are coupled in a single model. This model is restricted to
109 isotropic stress state only. This model has advantages over the previous models. The first
110 stress variable that was used by Wheeler et al. (2003) in their proposed framework is:

111 $$\sigma_{ij}^{*} = \sigma_{ij} - \left[S_r u_w + (1 - S_r) u_a\right]\delta_{ij} \qquad (1)$$

112 where σ_{ij}^{*} is Bishop' stress tensor (named by Bolzon et al. 1996), σ_{ij} is the total stress
113 tensor, S_r is degree of saturation, u_a and u_w are pore air and pore water pressures and
114 δ_{ij} is the Kroneker's delta. Since the Bishop's stress does not show the stabilizing effect
115 provided by the existence of meniscus water lenses, a second stress variable was
116 introduced to represent the effect of meniscus water. The second stress state variable, so
117 called modified suction, is defined as:

118 $$s^{*} = ns = n(u_a - u_w) \qquad (2)$$

where s^* is modified suction, n is porosity and s is suction. The modified suction was selected in combination with Bishop's stress tensor by considering the work input for unsaturated soil that was suggested by Houlsby (1997). Houlsby (1997) presented a comprehensive theoretical analysis of the work input to an unsaturated soil and showed the following equation:

$$p^* = p - S_r u_w - (1 - S_r)u_a = \bar{p} + S_r.s \quad (3)$$

where p^* is the mean Bishop's stress, and p, $\bar{p}$ and s are mean stress, mean net stress and suction respectively . They stated that p^* is influenced by increment of degree of saturation $-dSr$ but s^* is influenced by strain variable $d\varepsilon_v$ (increment of volumetric strain).

The above model was originally presented for isotropic stress state. Later it was extended to general stress state by Lloret-Cabot et al. (2013, and 2017). Lloret-Cabot et al. (2017) showed that the model proposed by Wheeler et al. (2003) can be used for triaxial loading conditions (anisotropic stress state). They suggested that it is necessary to consider mean Bishop' stress (p^*) and modified suction s^* as defined above, and deviator stress q:

$$q = \sigma_1 - \sigma_3 \quad (4)$$

where σ_1 and σ_3 are major and minor principal total stresses.

Critical state

The critical state theory was originally developed for saturated soils as a three-dimensional approach to modelling of soil behavior. It is defined in terms of three variables: mean net stress $\bar{p}$ ($p - u_w$), deviator stress q ($\sigma_1 - \sigma_3$) and specific volume v(1+e) (Schofield and Worth 1968).

141 The critical state framework for unsaturated soil has been studied and compared with that
142 for saturated soil by many researchers such as Alonso et al. (1990), Toll (1990), Wheeler
143 and Sivakumar (1995), Lloret and Khalili (2002), Toll and Ong (2003), Khalili et al.
144 (2004), Estabragh and Javadi (2008), Tarantino (2007) and Jotisankasa et al. (2009).
145 Alonso et al. (1990) proposed the following expression for deviator stress q and mean net
146 stress $\bar{p}$ ($p - u_a$) at critical state:

147 $$q = M\bar{p} + Mks \qquad (5)$$

148 where M is the slope of the critical state line for saturated soil. In the model of Alonso et
149 al. (1990), a single value of M was assumed for critical state lines for different values of
150 suction. Mk is the slope of the critical state line on a plane with constant $\bar{p}$ and s is
151 suction.
152 Toll (1990) conducted a number of triaxial tests on unsaturated compacted Kiuyn gravel
153 sand at constant water content. He suggested, based his results, that the critical state for
154 unsaturated soils could be expressed in terms of deviator stress, q, effective mean net
155 stress, $\bar{p}$, suction, s ($u_a - u_w$), specific volume, v and degree of saturation, S_r. Wheeler
156 and Sivakumar (1995) performed five different types of triaxial tests on unsaturated
157 compacted samples of kaolin. They presented critical state relationships for q and v which
158 took the form:

159 $$q = M(s)\bar{p} + \mu(s) \qquad (6)$$

160 $$v = \Gamma(s) - \psi(s)\ln\frac{\bar{p}}{p_{at}} \qquad (7)$$

161 where $M(s)$ is the slope of the critical state line at a specific suction and $\mu(s)$ is the
162 apparent cohesion or intercept caused by suction. $\Gamma(s)$ and $\psi(s)$ are intercept and the

slope of critical state line in $v:\ln \overline{p}$ space. The parameters $M(s)$, $\mu(s)$, $\Gamma(s)$ and $\psi(s)$ are all functions of suction. Maătouk et al. (1995) performed drained triaxil tests on unsaturated silty soil under different suctions. They found that the critical state lines in the plane of deviator stress and mean net stress are not parallel and converge to a point. Wang et al. (2002) conducted suction controlled triaxial drained tests on an unsaturated silty soil. They found that the critical state lines for unsaturated soil corresponding to different suctions are parallel to that of saturated soil in the planes of deviator stress against mean net stress or specific volume against mean net stress. Toll and Ong (2003) conducted constant water content triaxial tests on unsaturated soil and consolidated drained triaxil tests on saturated samples of sandy clay. They concluded that the parameters of critical state relationships are dependent on the degree of saturation of the soil. Estabragh and Javadi (2008) studied the critical condition for overconsolidated unsaturated silty soil through experimental tests. They found that the critical state lines are not parallel in the plane of deviator stress and mean net stress for different suctions and merge with each other. Jotisankasa et al. (2009) conducted controlled suction triaxial tests on loosely compacted soil samples that were composed of silt, kaolin and London clay. They showed the parameters of the critical state relationships are similar to the model that was proposed by Toll (1990). Lloret-Cabot et al. (2017) proposed a model that includes three yield surfaces in $\overline{p}:q:s^*$ space that are mechanical (M) yield surface used to describe the occurrence of plastic volumetric strains (mechanical behavior) potentially occurring during loading, yielding on the wetting retention yield surface WR corresponding to plastic increases in S_r, and yielding on the drying retention surface DR corresponding to plastic decreases in S_r. The assumption of the unique critical state line in

186 the $q : \overline{p}$ space had been confirmed by the Gallipoli et al. (2008) and Lloret-Cabot et al.
187 (2013).

188 *Aim of this work*

189 A review of the literature shows that the majority of the relationships and models for
190 unsaturated soils have been developed based on the study of mechanical behavior of soils
191 under drying paths. The shear strength and critical state of a soil under drying and wetting
192 conditions may be not the same. The shear strength of a soil under wetting condition is
193 one of the main problems in practical applications. Most of the slope failures are caused
194 by rainfall. Infiltration of rainwater to the soil creates a wetting front that leads to the
195 increase in pore water and reduction in matric suction. This causes the soil state to change
196 from drying path to wetting path. Subsequently the shear strength of soil changes from
197 drying to wetting behavior. This in turn results in a decrease in shear strength on the
198 potential failure surface to a point when equilibrium can no longer be sustained in the
199 slope and then failure occurs. However, there is very limited information on the
200 mechanical properties of unsaturated soils during wetting paths and particularly in
201 transition from drying to wetting. It is therefore necessary to understand the critical state
202 on wetting and to be able to assess the stability of soil during rainfall. The aim of this
203 research work is to study the critical state behavior of a soil during drying and wetting at
204 different suctions through a series of triaxial tests. The procedure of tests and the results
205 are presented and comparison is made between the critical state on drying and wetting
206 paths.

207 **Experimental study**

208 *Soil properties*

209 The soil used in the testing program was a silty soil with low plasticity, comprising 35%
210 sand, 53% silt and 12% clay. It had a liquid limit of 34% and plasticity index of 2%. The
211 soil can be classified as ML (silt with low plasticity) according to the Unified Soil
212 Classification System (USCS). The optimum water content in the standard compaction
213 test was 16.0% and the maximum dry unit weight was 15.0 kN/m^3.

214 *Sample preparation*

215 The slurry method was selected for preparing the samples for testing. Saturated samples
216 were used by some other researchers such as Rahardjo et al. (2004) and Thu et al. (2007).
217 In this method, the prepared slurry was compressed in a special mould by loading (details
218 can be found in Estabragh et al. 2017). The compressed samples were then taken from the
219 consolidation mould by using a number of thin walled stainless steel tubes with diameter
220 of 38 mm. Both ends of the extruded samples were sealed and they were kept in a
221 controlled temperature of 20^{o}C ± 1 before being used in the main tests. The initial
222 specific volume, degree of saturation and water content of the prepared samples were
223 1.62, 93.0% and 22.0 respectively.

224 *Experimental apparatus*

225 A double-walled triaxial cell was used for conducting the tests on unsaturated soil
226 samples under specific suction. The general layout of the used apparatus is shown in
227 Fig.1. The required pressures for the inner cell, outer cell and back pressure are provided
228 by three pressure control units. Each of these units was equipped with a servomotor for
229 controlling the applied pressure. Two Imperial College type volume change measurement
230 systems were used for measuring the flow of water in or out of the inner cell and sample.
231 The pore air pressure was applied to the sample from the top through a low air entry disk

and pore water pressure at the base through a high air entry disk with air entry value of 500 kPa (Fig.1). The axis translation technique was used for creating the desired suction in the sample by keeping the pore water pressure above the atmospheric pressure. A flushing system was used in the apparatus to prevent from accumulation the air bubbles beneath the high air entry disk. All the units of the apparatus were operated by a computerized program and logging system.

EXPERIMENTAL PROCEDURE

A program of experimental tests was designed and carried out to examine the effect of hydraulic hysteresis on the shear strength and critical state behavior of the silty soil. The tests were conducted on samples with suctions 0, 100, 200, 250 and 300 kPa on both dry and wet paths of soil water characteristic curve (Fig.2). The main stages of the experimental tests were equalization, consolidation and shearing. In addition, the soil water characteristic curve was obtained by conducting cyclic drying and wetting tests on the sample. The test procedures were as follows:

Equalization

Fig.3 shows the stress path, plotted as suction against mean net stress ($\bar{p}$) for equalization and ramped consolidation for the drying and wetting paths. Before conducting consolidation tests, the desired suction was created in the sample at the equalization stage. Therefore, the first stage of each test, after setting up the sample in the triaxial cell was equalization where the desired suction was created in the sample. As shown in Fig.3 the initial suction of sample was zero (point A at Fig.3) and the initial pressures of the two cells, air pressure and back pressure were set to 10, 6 and 5 kPa respectively. In order to bring the initial suction of sample to the desired value (0, 100,

200, 250 or 300 kPa) on drying path (Fig.3a) the target pressures of two cells and back pressure were set in the control software for the triaxial system to reach the target values at a prescribed time. The rate of 1.6 kPa/min was chosen for increasing pressure from their initial values to the target values (6 kPa/hour was used by Thu et al., 2007 and 4 kPa/hour by Vassalo et al., 2007 for samples of silty soil). For the wetting path, the initial suction of each sample was brought to 300 kPa (Fig.3b) and it subsequently followed the desired suction (250, 200, 100 or 0 kPa). During equalization, the volumes of water inflow or outflow from the inner cell and sample were continuously recorded. The duration of equalization was between 5 and 8 days depending on the target suction. The equalization stage was terminated when the flow of water decreased to less than 0.1 cm^3/day (as used by Sivakumar, 1993 and Sharma, 1998).

Determination of soil water characteristic curve

The purpose of this test was to determine the air entry value of the soil. The soil water characteristic curve was established after equalizing the sample at the suction of 20 kPa. The air pressure and cell pressure were kept constant (350 and 370 kPa respectively) and pore water pressure was decreased with a rate of 0.5 kPa/h (as used by Khalili and Zargarbashi, 2010) until it reached 50 kPa. During this process the drying curve was established so, the suction at the end of the drying path was 300 kPa. For the wetting section, the air and cell pressures were kept constant and pore air pressure was increased at the same rate as drying. It was continued until 300 kPa. The soil water characteristic curve was established based on the degree of saturation and specific volume (Fig.4). As shown in Fig.4a the degree of saturation at suction of 20 kPa was about 98%. By increasing suction the degree of saturation decreased so, at suction of 300 kPa the value

278 of it was 41.0%. By decreasing suction the degree of saturation increased and at suction
279 of 30 kPa it reached 81.8%. Fig.4b shows that the value of specific volume at drying and
280 wetting paths is not the same. At the initial drying path, the specific volume was 1.62 and
281 at the end of this path it reached to 1.46 but at wetting path this value (1.46) was
282 increased until it reached to 1.53. It is resulted that during drying and wetting not only the
283 degree of saturation but also the specific volume at the same suction are not the same.
284 The air entry value was found from Fig.4a to be about 60 kPa by using the method that
285 was proposed by Vanapalli et al. (1999).

286 *Consolidation*

287 After the sample was equalized at a specified suction (0, 100, 200, 250 or 300 kPa on dry
288 or wet path of SWCC) and mean net stress (20 kPa), it was isotropically loaded by
289 increasing the mean net stress to a preselected target value (usually 550 kPa) while
290 holding the suction constant (air pressure and water back pressure were kept constant)
291 (Fig.3). The method of ramping load was used to conduct consolidation. For
292 consolidation, the initial and target values of cell pressures and the time to achieve the
293 target values were set in the computer program. At the end of each test, the sample was
294 left under the target pressures for 24 hours to ensure of dissipation of any excess pore
295 water pressure. During this stage each sample was consolidated to a virgin state.

296 *Shearing*

297 Drained shear tests were conducted under constant cell pressure at a constant rate of axial
298 strain on samples that were consolidated to a virgin state. The rate of 0.12mm/hour was
299 chosen for axial displacement in the shearing tests (giving a strain rate of about 3.78%
300 per day as used by Cui and Delage (1996) and Sivakumar (1993)). This rate was used to

ensure the dissipation of excess pore water pressure during the test. The variations of the volume of sample were calculated from the recorded values the volume of inflow or outflow water from the inner cell. The variations of mean net stress, deviator stress, axial volumetric strains, and degree of saturation (S_r) were calculated from the recorded data. All the samples were tested to the critical state at the end of shearing stage where deviator stress (q), mean net stress ($\bar{p}$) and specific volume (v) either remained constant or changed very slowly.

RESULTS

Equalization

During the equalization stage, the variations of specific volume, degree of saturation and specific water volume were recorded with time. For creating suctions of 0, 100, 200, 250 or 300 kPa they were reduced from their initial values as shown in Table.1. By increasing the suction from its initial value to desired values of 0, 100, 200, 250 or 300 kPa the outflow of water from the sample was increased and specific volume was decreased. Table 1 shows that for the suction of 0 kPa, the direction of the flow of water was into the sample while for the rest of the suctions the water flow was out of the samples**.** The final variations of specific volume, degree of saturation and specific water volume for suctions of 250, 200, 100 and 0 kPa for the samples on the wetting path are also shown in Table 1. The equalization for the wetting path consisted of two stages; in the first stage the suction of 300 kPa was created in the sample and then it was reduced to a predefined suction (250, 200, 100 or 0 kPa). The variations of specific volume are made of two stages; in the first stage the specific volume was reduced but in the next stage it was increased until it reached to equilibrium state as was indicated by Estabragh et al. (2017). Table 1 shows

the final values of specific volume, degree of saturation and specific water volume at the end of equalization for specific suctions on the wetting path of the soil water characteristic curve.

Consolidation and shearing

During ramp consolidation the mean net stress ($\bar{p}$) was increased from its initial value (20 kPa) to target value (550 kPa) under constant suction of 0, 100, 200, 250 or 300 kPa on the drying path and at suctions of 300, 250, 200, 100 or 0 kPa on the wetting path. The variations of specific volume (v), degree of saturation (S_r) and specific water volume (v_w) with mean net stress $\bar{p}$ during ramped consolidation were recoded. The values of pre-consolidation pressure, p_c (yield stress) for different suctions for both drying and wetting paths, along with specific volume and degree of saturation at the end of consolidation are shown in Table 1.

A total of 36 controlled suction drained triaxial shear tests with constant cell pressure were performed on normally consolidated samples on the drying and wetting paths of the soil water characteristic curve (see Table 2). In this test program, four cell pressures of 100, 200, 300 and 400 kPa at suctions 0, 100, 200, 250 and 300 kPa for the drying path and 100, 150, 200 and 300 kPa at suctions 250, 200, 100 and 0 kPa for the wetting path were used. All the shearing tests reached the critical state condition with no evidence of any obvious peak in the curve, and the samples failed by barreling in a plastic fashion rather than by the formation of a distinct failure plane. Typical results of shearing tests for various suctions on the dry and wetting paths are presented below:

The results of the shear tests at suction of 0 kPa are shown in Fig.5. As shown in Fig.5a, in the test with cell pressure of 100 kPa, the deviator stress increased until it reached a

maximum value of about 46 kPa at strain of 4.6% after which, it remained nearly constant. During this stage, dilation occurred in the sample. In the other tests with cell pressures of 200, 300 and 400 kPa, the deviator stress increased up to axial strains of 11.4%, 10% and 7.32% respectively and then remained nearly constant. As shown in Fig5b, contraction occurred in all of these samples during shearing and the amount of contraction increased with increasing the cell pressure. Typical results at suction of 200 kPa and different cell pressures (100, 200 and 300 kPa) are shown in Fig. 6. As shown in Fig.6a, at cell pressures of 100, 200 and 300 kPa the maximum deviator stresses are 216, 290 and 362 kPa for the dry side and 360, 379 and 418 kPa on the wet side respectively. The volumetric strains at cell pressures of 100, 200 and 300 kPa are 0.317, -3.9 and -6.41% on the dry side and 0.457, -2.01 and -3.21% on the wet side respectively (Fig.6b). It is seen from Fig.6c that, for the shearing tests under cell pressures of 100, 200 and 300 kPa on the drying path, the degrees of saturation are less than those for the same cell pressures on the wetting path.

Discussion

The results of the shearing tests in Table 2 show that during the test, at cell pressure of 100 kPa, the volume of the samples increased and the degree of saturation decreased on both the drying and wetting paths. The amounts of increase in volume and decrease in S_r at this cell pressure were dependent on the value of suction. It is also observed from this table that, for this cell pressure, the degree of dilation is increased and S_r is decreased with increasing suction. The dilation is likely due to the fact that higher suctions result in more tightly bound aggregates that do not shear easily, rather tend to roll over each other (dilation) as shear stresses are increased. It can be concluded that the increase in the

volume between the particles during shearing leads to the reduction of S_r. The tendency to dilation and reduction of S_r is most pronounced at this cell pressure (100 kPa) and higher applied suctions, but at higher cell pressures and lower suctions, the volume change behavior during shearing is dominated by compression and results in increase in S_r because of the reduction in the pore spaces between particles. This behavior is consistent with the results that were reported by Cui and Delage (1996) and Houston et al. (2008). By increasing the cell pressure at the same suction, the volume change curves show a progressive evolution from dilative to compressive behavior with increasing the cell pressure that results in increase in degree of saturation. At the same cell pressure and different suctions, the amounts of contraction and increase in S_r are dependent on the suction; higher contraction and increase in S_r are observed at lower suctions for both drying and wetting paths.

Comparison of the results shows that at the same suction, the deviator stress-axial strain, volumetric strain-axial strain and degree of saturation-axial strain curves (Table 2) are not the same on the drying and wetting paths, and same cell pressure. At the same axial strain, the values of deviator stress on the wetting path are more than the drying path, the amount of contractive volumetric stain is less on the wetting path than the drying path but the variations degree of saturation is more on the wetting path than the drying path. Similar results can be observed in Table 2 for suctions 0, 100 and 250 kPa. This can be attributed to the value of void ratio or specific volume (in other word dense or loose condition of the samples) before shearing. The results of the consolidation tests show that the pre-consolidation (yield stress) pressures of the samples on the wetting path are more than the drying path and the slopes of normal consolidation lines for the wet samples are

393 less than the dry ones at the same suction (Table 1). Also at the same suction, the values
394 of void ratio at the end of consolidation for the samples on the wetting path are less than
395 the samples on the drying path (Table 1). It is concluded that the samples on the wetting
396 path are denser and more compressed than the samples on the dry path as suggested by
397 Estabragh et al. (2017).
398 In the hysteresis phenomenon, the degree of saturation is important (see equations 1 and
399 3). The value of p^* was calculated at critical state condition by using p^* and S_r at
400 critical state for each applied suction and cell pressure for the drying and wetting paths
401 (see eq.3). The results of critical state data are shown in Fig. 7 in the $q:p^*$ plane for the
402 constant suction shear tests performed at suctions of 0, 100, 200, 250 and 300 kPa for dry
403 and wet paths. Comparison of the results shows that for suctions of 100, 200 and 250 kPa,
404 the values of $M(s)$ are slightly less on the wetting path than the drying path (Table 3). If
405 the values of $M(s)$ for suctions 100, 200 and 250 kPa are rounded up, the lines for
406 suctions of 100, 200, 250 and 300 would be nearly parallel to each other on both dry and
407 wet paths. The values of $M(s)$ on the dry path are 0.40, 0.50, 0.50, 0.51 and 0.53 for
408 suctions 0, 100, 200, 250 and 300 kPa respectively (Table 3). It is resulted from table 3
409 that on the drying path, at all suctions except s= 0, the critical state lines are parallel. On
410 the wetting path, the values of $M(s)$ are 0.42, 0.45, 0.46 and 0.48 for suctions of 0, 100,
411 200, 250 and 300 kPa respectively (Table 3). Therefore, on the wetting path, the critical
412 state lines at different suctions are nearly parallel to each other and to the critical state
413 lines on the drying path. It is also observed that the values of $\mu(s)$ on the wetting path
414 are more that the similar values on the drying path. As mentioned above, the degree of

saturation has an important effect on the fabric of soil. This difference of fabric may be due to the different degrees of saturation causing different fabrics in the soil.

Fig. 8 shows the critical state values of specific volume (v) plotted against p^* (with p^* on logarithmic scale) for constant suction shear tests conducted at suctions of 0, 100, 200, 250 and 300 kPa on the dry and wet paths. The critical state values of v appear to fall on a unique critical hyperline (i.e., a unique line for each value of suction). Inspection of Fig. 8 indicates that the critical state lines for both paths are in the form of equation 7 and the position of them is similar to the consolidation curves in the v: Ln $\bar{p}$ space (Estabragh et al., 2017). Tables 1 and 3 show the consolidation and critical state parameters of the soil for the drying and wetting paths. The results show that the slopes of the critical state lines ($\psi(s)$) and the normal consolidation lines ($\lambda(s)$) are not the same (Tables 1 and 3). The trend of variation of $\psi(s)$ is increasing with suction until suction of 200 kPa and then there is a reduction in the value of it with further increase in suction. These variations of $\psi(s)$ with suction are not similar to the variations of $\lambda(s)$ with suction. These results are supported by the findings that were presented by Jotisankasa et al. (2009) who argued that the values of degree of saturation change along each line which causes them not to be parallel. Inspection of the data in Table 3 shows that the values of $\psi(s)$ for the wetting path are less than the drying path. This trend is also similar to the variations of $\lambda(s)$ for the wetting and drying paths (Table 1). The results show that the values of $\Gamma(s)$ for the range of suctions used in this work are nearly the same for the drying path, except for suction of 300 kPa. The value of $\Gamma(s)$ on the drying path is more than the wetting path. The results in Table 3 show that the trend of variations of $\Gamma(s)$ with suction is not the

437 same as $N(s)$ because the value of $N(s)$ is decreased with increasing suction for both
438 paths (Table 1).
439 The data obtained for samples at critical state condition with different suctions on both
440 dry and wet conditions were also examined with equations 6 and 7. Table 3 shows the
441 final values of the critical parameters that were obtained by using these relationships
442 (condition b). As shown in the table, the values of *M(s)* for different suctions (except s=0)
443 are the same but the values on wetting path is slightly less than the dry path. The values
444 of $\mu(s)$ are increased with increasing suction on both paths. The variations of $\psi(s)$ with
445 suction are similar to *M(s)*. $\Gamma(s)$ is also decreased with increasing suction at both drying
446 and wetting paths. Comparing the results in Table 3 (at conditions a and b) shows that the
447 values of some parameters such as $\mu(s)$ and $\psi(s)$ that were obtained by equations 6 and 7
448 (proposed by Wheeler and Sivakumar 1995) are not the same as the parameters that were
449 calculated based on equation 3. This difference could be due to the different equations
450 that were used; the results in condition a (Table 3) are based on equation 3 which
451 includes the degree of saturation. It can be said that the data in this condition in Table 3
452 are more reliable as the degree of saturation has important role in hydraulic hysteresis and
453 should be considered in critical state condition.
454 **Conclusion**
455 The effect of hydraulic hysteresis on the shear strength and critical state behavior of an
456 unsaturated silty soil was studied through a comprehensive set of triaxial tests. The
457 following conclusion can be drawn from the results of this study.
458 - At high cell pressures, contraction and increase in degree of saturation are
459 observed in the sample during shearing. At a constant suction the amounts of

contraction and degree of saturation are increased with increasing cell pressure. At a constant cell pressure the amount of contraction is reduced with increasing suction. The contraction and increase in degree of saturation of samples are less on the wetting path than the drying path.

- Critical state condition exists for both dry and wet paths but the critical values of q, p^* and v or q, $\bar{p}$, v for the dry and wet paths at different suctions are not the same. This could be attributed to the effect of hysteresis due to the different degrees of saturation of samples at critical state.
- The parameters $M(s)$, $\mu(s)$, $\psi(s)$, $\Gamma(s)$ that define the critical state lines in the q: p^* and v: Ln p^* or q: $\bar{p}$ and v: Ln $\bar{p}$ spaces are not the same for the dry and wet paths.

Data Availability

Some or all data, models, or code generated or used during the study are available from the corresponding author by request (list items).

References

Alonso, E.E., Gens, A. and Josa, A. (1990). "A constitutive model for partially saturated soil." *Géotechnique,* 40(3), 423–439.

Bolzon, G., Schrefler, B.A. and Zienkiewicz, O.C. (1996). "Elastoplastic soil constitutive laws generalized to partially saturated states." *Géotechnique,* 46(2), 279-289.

Buisson, M.S.R. and Wheeler, S.J. (2000). "Inclusion of hydraulic hysteresis in a new elasto-plastic framework for unsaturated soils." *Proc., Int. Workshop, unsaturated soils*, Trento, 109-119.

Cui, Y.J. and Delage, P. (1996). "Yielding and plastic behavior of an unsaturated compacted silt." *Géotechnique*, 46(2), 291–331.

Estabragh, A.R. and Javadi, A.A. (2008). "Critical state for overconsolidated silty soil." *Can. Geotech. J.*, 45, 408-420.

Estabragh, A.R., Moghadas, M. and Javadi, A.A. (2017). "Consolidation behavior of an unsaturated silty soil during drying and wetting." *Soil Found*, 5(2), 277-287.

Farias, M.M., Pinheiro, M. and Neto, M.P.C. (2006). "An elastoplastic model for unsaturated soils under general three-dimensional condition." *Soil Found*, 46(5), 613-628.

Gallipoli, D., Gens, A., Chen, G. and Donza, F. (2008). "Modeling unsaturated soil behavior during normal consolidation and at critical state." *Comput Geotech*, 35(6), 825-834.

Gallipoli, D., Gens, A., Sharma, R. and Vaunat, J. (2003). "An elasto-plastic model for unsaturated soil incorporating the effects of suction and degree of saturation on mechanical behavior." *Géotechnique*, 53(1), 123-135.

517 Guan, G.S., Rahardjo, H. and Choon, L.E. (2010). "Shear strength equations for
518 unsaturated soil under drying and wetting." *J. Geotech. Geoenviron. Eng.,* 136,
519 594-606.
520 Houlsby, G.T. (1997). "The work input to an unsaturated granular material."
521 *Géotechnique*, 47(1), 193-196.
522 Houston, S.L., Perez-Garcia, N. and Houston, W.N. (2008). "Shear strength and shear-
523 induced volume change behavior of unsaturated soils from a triaxial test
524 program." *J. Geotech. Geoenviron. Eng.,* 134(11), 1619-1632.
525 Jommi, C. (2000). "Remarks on the constitutive modeling of unsaturated soils." *Proc., Int.*
526 *Workshop, unsaturated soils*, Trento, 139-153.
527 Jotisankasa, A., Coop, M. and Ridely, A. (2009). "The mechanical behavior of an
528 unsaturated compacted silty clay." *Geotéchnique*, 59(5), 415-428.
529 Khalili, N., Geiser, F. and Blight, G.E. (2004). "Effective stress in unsaturated soils:
530 Review with new evidence." *Int. J. Geomech.*, ASCE, 4(2), 115-126.
531 Khalili, N. and Zargarbashi, S. (2010). "Influence of hydraulic hysteresis on effective
532 stress in unsaturated soils." *Géotechnique*, 60(9), 729–735.
533 Khosravi, A., Rahimi, M., Gheibi, A., and Shahrabi, M.M. (2018)."Impact of Plastic
534 Compression on the Small Strain Shear Modulus of Unsaturated Silts." *Int. J.*
535 *Geomech*., 18(2), 04017138-12.
536 Khoury, C.N. and Miller, G.A. (2012). "Influence of hydraulic hysteresis on the shear
537 strength of unsaturated soils and interfaces." *Geotech. Test. J*., 35(1), 1-15.
538 Li, W. and Yang Q. (2018)." Hydromechanical Constitutive Model for Unsaturated Soils
539 with Different Overconsolidation Ratios." *Int. J. Geomech*., 18(2),04017142-1, 16

Li, X.S. (2005). "Modelling of hysteresis response for arbitrary wetting/drying paths." *Comput Geotech*, 32(2), 133-137.

Lloret, B. and Khalili, N. (2002). "An effective stress elastic-plastic model for unsaturated porous media." *Mech. Mater.*, Elsevier, 34(2), 97-116.

Lloret-Cabot, M., Sánchez, M. and Wheeler, S.J. (2013). "Formulation of a three-dimensional constitutive model for unsaturated soils incorporating mechanical – water retention coupling." *Int. J. Numer. Anal. Methods. Geomech.*, 37, 3008-3035.

Lloret-Cabot, M., Wheeler, S.J. and Sánchez, M. (2017). "A unified mechanical and retention model for saturated and unsaturated soil behavior." *Acta. Geotech.*, 12, 1-21.

Lu, N., Kaya, M., Collins, B.D. and Godt, J.W. (2013). "Hysteresis of unsaturated hydromechanical properties of a silty soil." *J. Geotech. Geoenviron. Eng*., 134(3), 507-510.

Maâtouk, A., Leroueil, S., and Larochelle, P. (1995). Yielding and critical state of a collapsible unsaturated silty soil. *Géotechnique*, 45(3): 465-477.

Másín, D. (2010). "Predicting the dependency of a degree of saturation on void ratio and suction using effective stress principle for unsaturated soils." *Int. J. Numer. Anal. Methods. Geomech*., 34, 73-90.

Nuth M. and Laloui, L. (2008). " Advances in modeling hysteretic water retention curve in deformable soils." *Comput. Geotech*, 35(6), 835-844.

561 Rahardjo, H., Heng, O.B. and Choon, L.E. (2004). “Shear strength of a compacted
562 residual soil from consolidated drained and constant water content triaxial tests.”
563 *Can. Geotech. J*., 41(3), 421-436.
564 Rojas, E., Chávez, O., Arroyo, H., López-Lara, T., Hernández, J.B. and Horta, J. (2017).”
565 Modeling the Dependency of Soil-Water Retention Curve.” *Int. J. Geomech*.,
566 17(1),
567 Schofield, A.W. and Worth, C.P. (1968). *Critical state soil mechanics*. McGraw-Hill,
568 Lonodon, U.K.
569 Sharma R.S. (1998). “Mechanical behaviour of unsaturated highly expansive clays.”
570 D.phil thesis, University of Oxford, Oxford, UK.
571 Sivakumar V. (1993). “A critical state for unsaturated soil.” Ph.D thesis, University of
572 Sheffield, Sheffield. UK.
573 Sun, D., Zhang, J, Gao, Y. and Sheng, D. (2016). “Influence of Suction History on
574 Hydraulic and Stress-Strain Behavior of Unsaturated Soils.” *Int. J. Geomech*.,
575 16(6),D4015001-9.
576 Tamagnini, R. (2004). “An extended Cam-clay model for unsaturated soils with
577 hydraulic hysteresis.” *Géotechnique*, 54(3), 223–228.
578 Tang, Y., Taiebat, H.A. and Russel, A. (2018).”Numerical Modeling of Consolidation of
579 Unsaturated Soils Considering Hydraulic Hysteresis.” *Int. J. Geomech*., 18(2),
580 04017136-23.
581 Tarantino, A. (2007). “A possible critical state framework for unsaturated compacted
582 soils.” *Géotechnique*, 57(4), 385-389.

583 Thu, T.M., Rahardjo, H. and Leong, E-C. (2007). "Soil-water characteristic curve and
584 consolidation behavior for a compacted silt." *Can. Geotech. J*., 44(3), 266-275.
585 Toll, D.G. (1990). "A framework for unsaturated soil behavior." *Géotechnique*, 40(1),
586 31-44.
587 Toll, D.G. and Ong, B.H. (2003). "Critical-state parameters for an unsaturated residual
588 sandy clay." *Géotechnique*, 53(1), 93-103.
589 Vanapalli, S.K., Fredlund, D.G. and Pufahl, D.E. (1999). "The influence of soil structure
590 and stress history on the soil-water characteristics of compacted till."
591 *Géotechnique*, 49(2), 143-159.
592 Vassalo P., Mancuso C. and Vinale F. (2007). "Effect of net stress and suction history on
593 the small strain stiffness of a compacted clayey silt." *Canadian Geotechnical*
594 *Journal*, 44 (4),447-462.
595 Vaunat, J., Romero, E. and Jommi, C. (2000). *An elastoplastic hydromechanical model*
596 *for unsaturated soils*. Tarantino, S., mancuso, C., ed., Experimental evidence and
597 theoretical approaches in unsaturated soils, Rotterdam, 121-138.
598 Wang, Q., Pufahl, D.E., and Fredlund, D.G. (2002). "A study of critical state on an
599 unsaturated silty soil." *Can. Geotech. J.,* 39, 213-218.
600 Wheeler, S.J. (1988). "The undrained shear strength of soils containing large gas
601 bubbles." *Géotechnique*, 38(1), 399–413.
602 Wheeler, S.J., Sharma, R.S. and Buisson, M.S.R. (2003), "Coupling of hydraulic
603 hystersis and stress-strain behavior in unsaturated soils." *Géotechnique*, 53(1), 41-
604 54.

Wheeler, S.J., Sivakumar, V. (1995). “An elasto plastic critical state framework for unsaturated soil.’’ *Géotechnique*, 45(1), 35-53.

Table 1. Specific volume (v), degree of saturation (S_r) and specific water volume (v_w) after equalization and Preconsolidation pressure (p_c) with consolidation parameters for different suctions on the drying and wetting paths

Condition	Parameters	Drying path					Wetting path			
		Suction (kPa)					Suction (kPa)			
		0	100	200	250	300	0	100	200	250
After equalization	v	1.62	1.57	1.51	1.50	1.37	1.53	1.52	1.50	1.48
	S_r (%)	97.0	80.0	66.33	61.0	42.32	83.47	65.1	61.0	42.3
	v_w	1.60	1.46	1.34	1.31	1.20	1.44	1.17	1.31	1.20
After consolidation	v	1.46	1.45	1.44	1.42	1.40	1.42	1.41	1.40	1.39
	S_r (%)	94.22	60.10	56.90	52.58	39.8	79.00	67.18	53.24	45.68
	v_w	1.43	1.27	1.25	1.22	1.16	1.33	1.27	1.21	1.18
Consolidation	p_c (kPa)	60	105	145	160	170	85	125	155	165
	$\lambda(s)$	0.077	0.067	0.061	0.059	0.057	0.067	0.063	0.059	0.058
	$N(s)$	1.95	1.87	1.82	1.78	1.75	1.84	1.81	1.78	1.77

679
680
681
682 **Table 2**. Final results of the drained triaxial tests carried out at different suctions under
683 various cell pressures for the drying and wetting paths

Condition	Suction (kPa)	Cell pressure (kPa)	$\overline{p}$ (kPa)	q (kPa)	ε_a (%)	ε_v (%)	ν	S_r (%)	v_w
Drying	0	100	115	46	6.97	0.16	1.576	72.0	1.41
		200	230	93	12.75	-4.49	1.530	73.6	1.39
		300	346	138	10.4	-6.96	1.492	72.1	1.35
		400	461.5	184	8.67	-9.27	1.470	56.6	1.30
	100	100	136	108	7.5	0.26	1.545	50.0	1.27
		200	265	194	9.21	-3.9	1.500	52.1	1.26
		300	384	250	10.52	-6.6	1.470	53.3	1.25
		400	497	290	10.92	-8.8	1.454	54.7	1.24
	200	100	173	216	6.97	0.317	1.512	47.0	1.24
		200	297	290	14.1	-3.9	1.478	49.6	1.24
		300	421	362	20.8	-6.41	1.445	51.8	1.23
		400	533	400	9.6	-8.08	1.40	51.2	1.20
	250	100	224	371	9.47	0.58	1.475	45.6	1.22
		200	352	454	12.75	-3.25	1.445	48.2	1.21
		300	470	510	20.8	-4.65	1.421	49.9	1.21
		400	586	560	15.26	-5.63	1.410	51.1	1.21
	300	100	280	540	13.0	0.8	1.415	34.3	1.14
		200	393	578	14.1	-2.21	1.40	34.8	1.14
		300	530	690	20.26	-2.78	1.385	35.5	1.14
		400	645	734	15.26	-4.8	1.375	35.9	1.13
Wetting	0	100	116	49	6.97	0.14	1.502	70.3	1.35
		150	176	77	12.6	-3.5	1.485	67.5	1.33
		200	233	99	10.13	-4.02	1.465	66.2	1.31
		300	349	147	8.67	-5.17	1.440	63.2	1.28
	100	100	167	201	7.5	0.23	1.475	57.0	1.27
		150	234	253	9.21	-2.3	1.456	58.3	1.26
		200	391	280	10.4	-3.66	1.439	59.9	1.26
		300	403.5	310	10.8	-4.86	1.422	61.1	1.26
	200	100	220	360	6.97	0.457	1.451	51.2	1.23
		150	280	379	15.25	-2.01	1.434	52.7	1.23
		200	340	418	20.13	-3.21	1.423	54.3	1.23
		300	456	470	9.07	-4.32	1.410	54.8	1.22
	250	100	269	509	9.47	0.50	1.433	42.8	1.19
		150	325	526	12.75	-1.84	1.419	44.0	1.18
		200	387	561.5	20.26	-3.01	1.411	44.6	1.18
		300	510	631	15.13	-3.87	1.392	46.0	1.18

684

Table 3. Critical state parameters at different suctions for the drying and wetting paths

Condition	Suction (kPa)	a- Critical state based on p^*				b- Critical state based on $\bar{p}$			
		$M(s)$	$\mu(s)$	$\psi(s)$	$\Gamma(s)$	$M(s)$	$\mu(s)$	$\psi(s)$	$\Gamma(s)$
Dry path	0	0.4	0.0	0.07	1.91	0.40	0.0	0.077	1.95
	100	0.5	26.5	0.085	1.92	0.52	50.0	0.071	1.90
	200	0.5	90.2	0.091	2.01	0.52	132.0	0.071	1.88
	250	0.51	205.0	0.085	1.97	0.52	252.0	0.066	1.83
	300	0.53	322.0	0.053	1.72	0.52	388.0	0.06	1.78
Wet path	0	0.42	0.0	0.064	1.83	0.43	0.0	0.056	1.76
	100	0.45	108.0	0.060	1.80	0.45	139.0	0.046	1.70
	200	0.46	209.0	0.056	1.76	0.48	251.0	0.042	1.66
	250	0.48	318.0	0.054	1.74	0.52	361.0	0.038	1.63

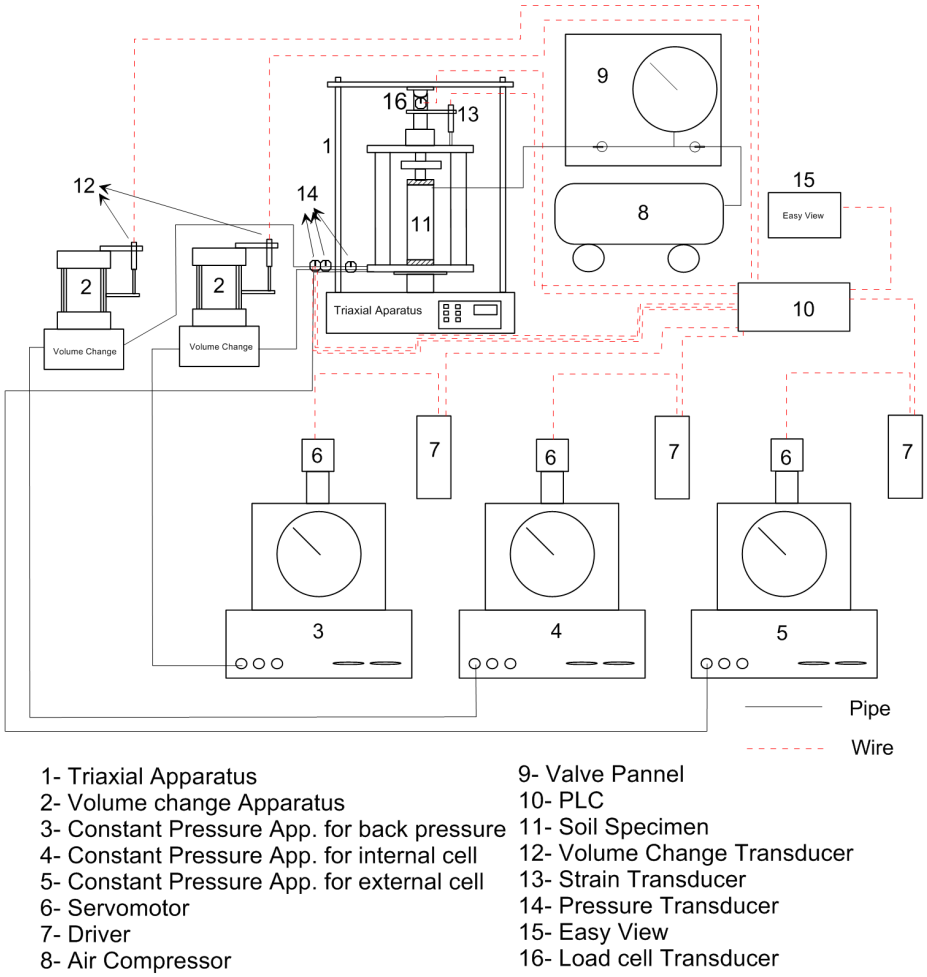

Fig.1. A general layout of the apparatus

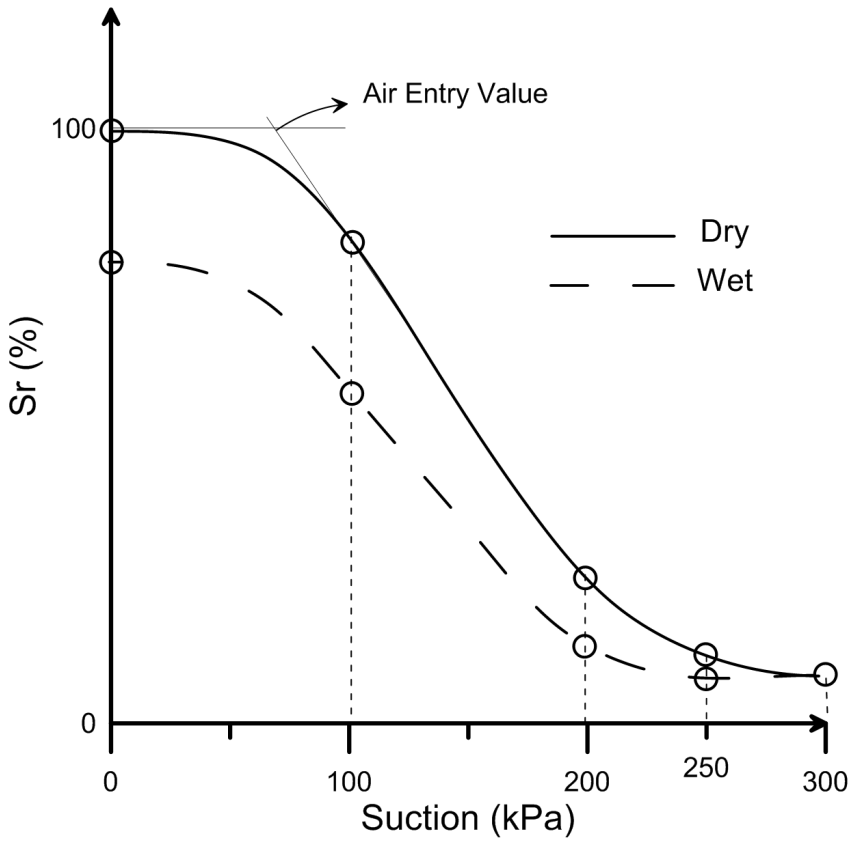

Fig.2. Selected suctions on the drying and wetting curves that were used in the test program

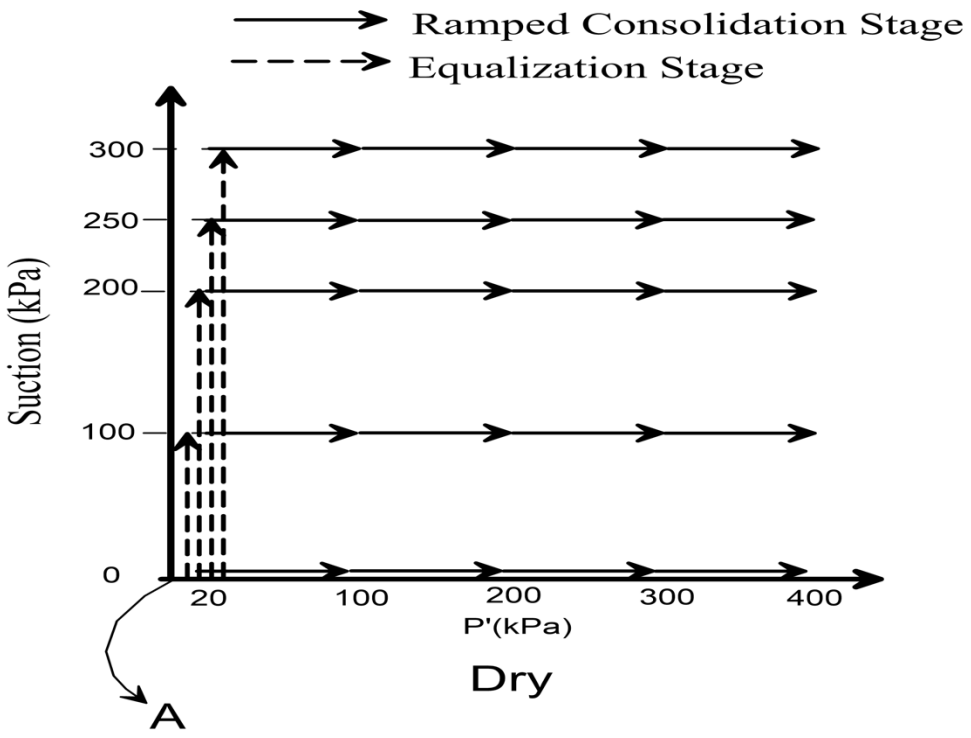

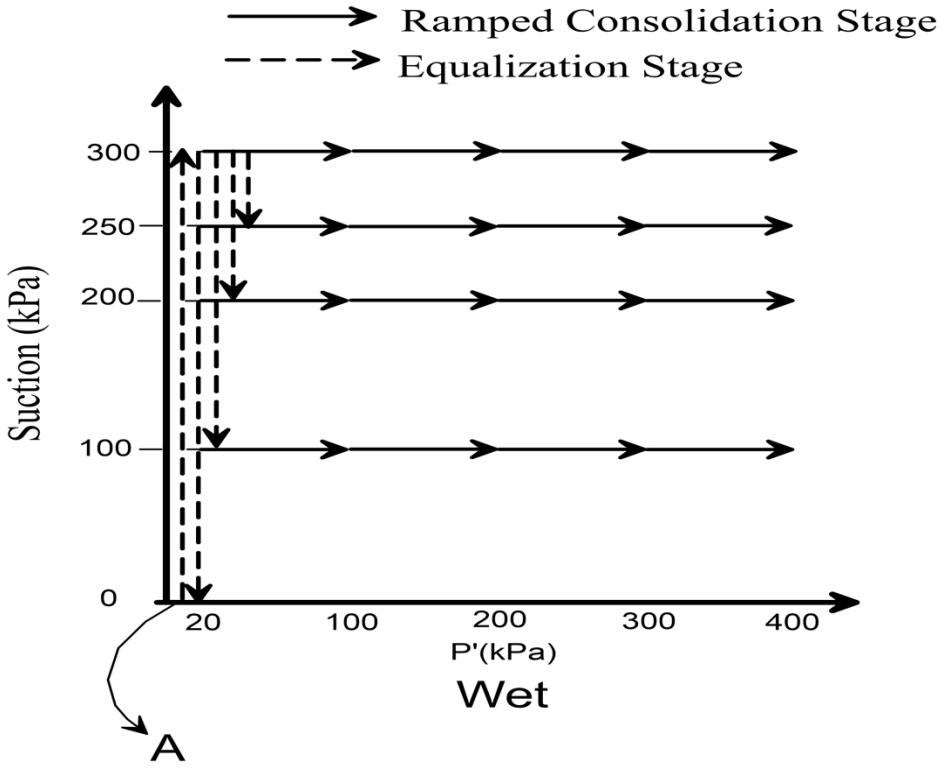

Fig.3. Stress paths during equalization and ramped consolidation (a) dry path, (b) wet path

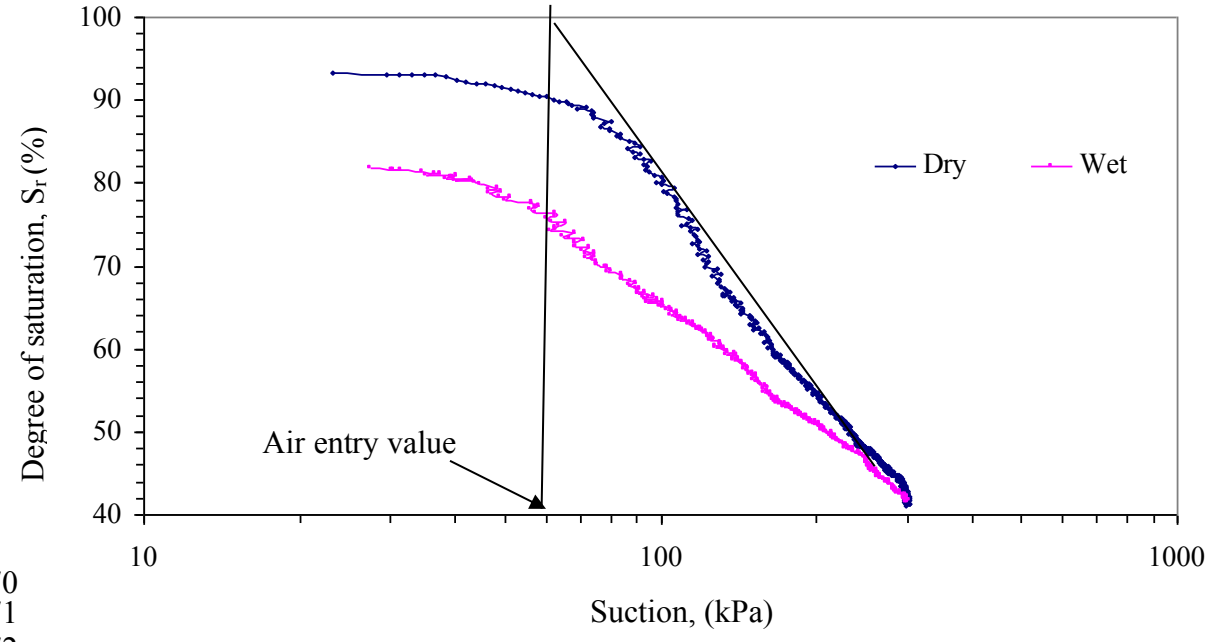

(a)

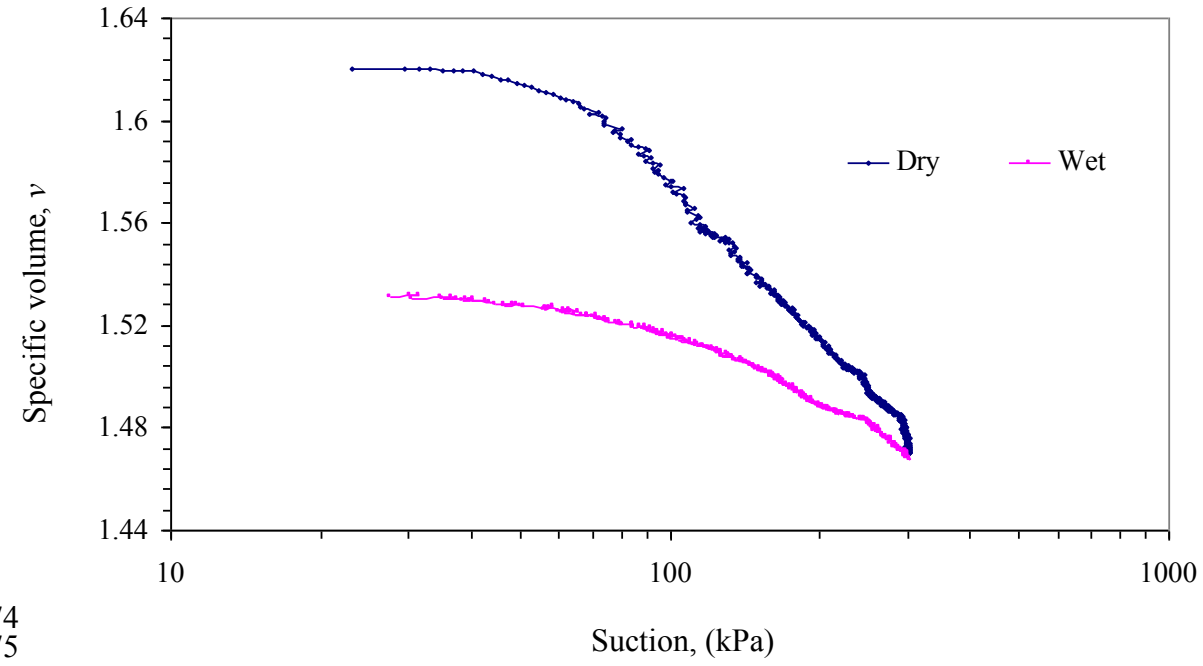

(b)

Fig.4. Soil water characteristic curves for drying and wetting paths (a) variation of S_r with suction (b) variation of υ with suction

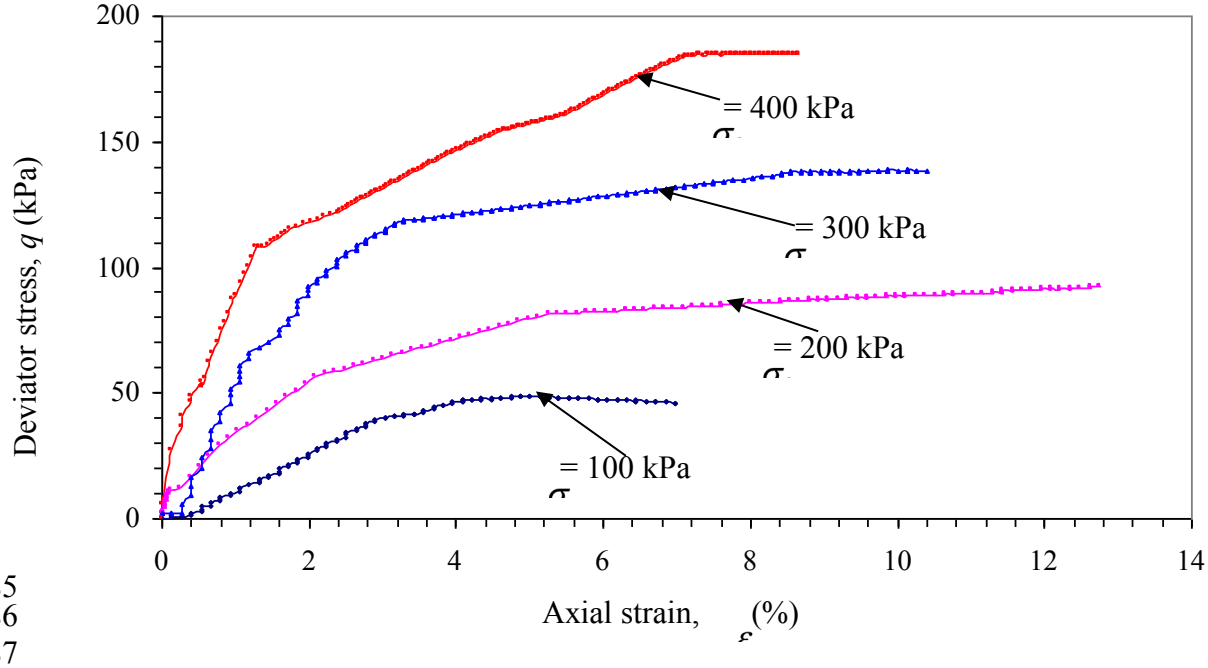

(a)

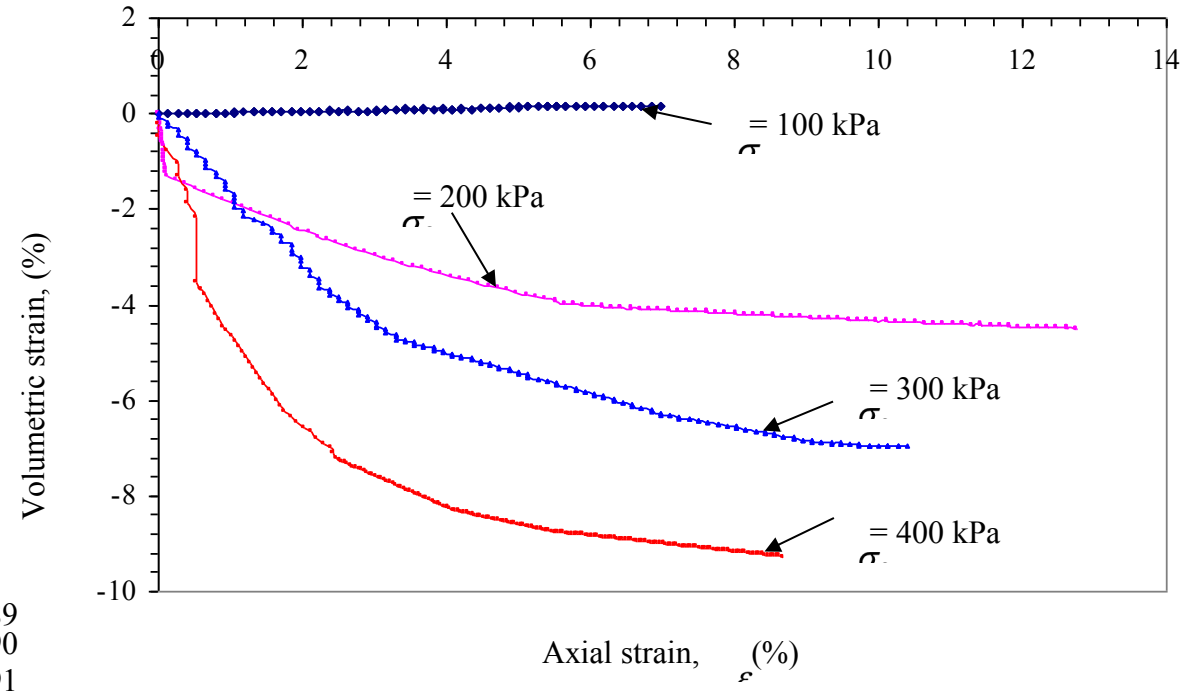

(b)

Fig. 5. Results for drained tests on samples with s =0 kPa, on the dry side: (a) deviator stress vs axial strain ; (b) volumetric strain vs axial strain.

797
798

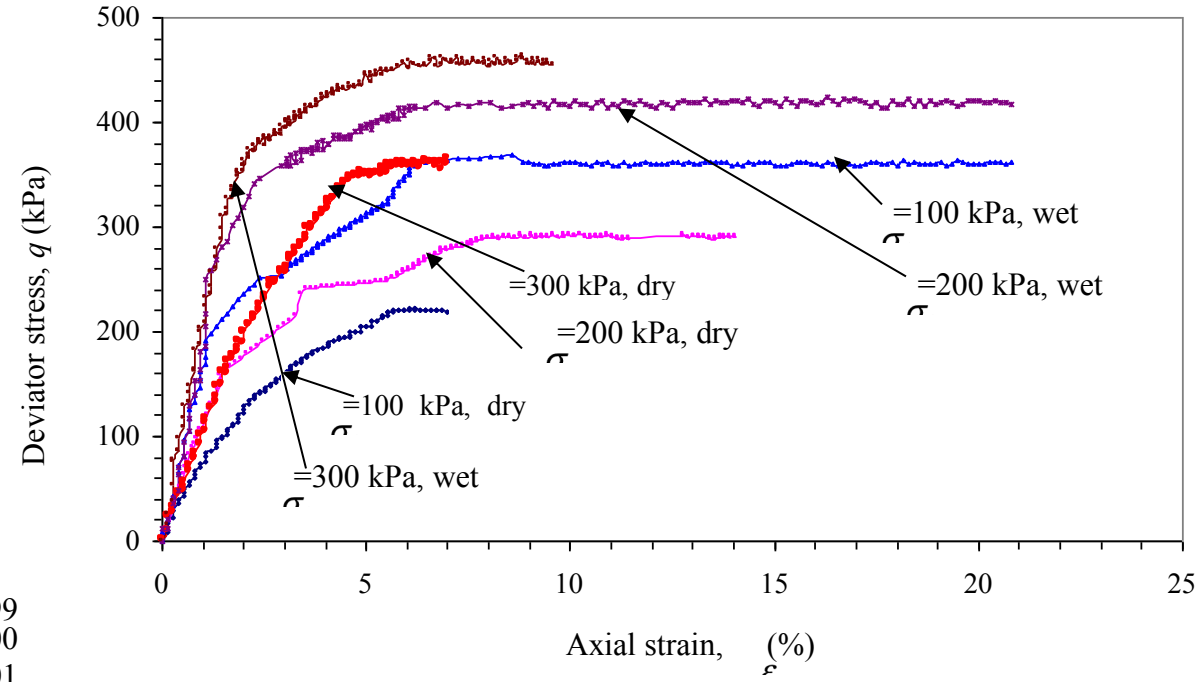

799
800
801
802

(a

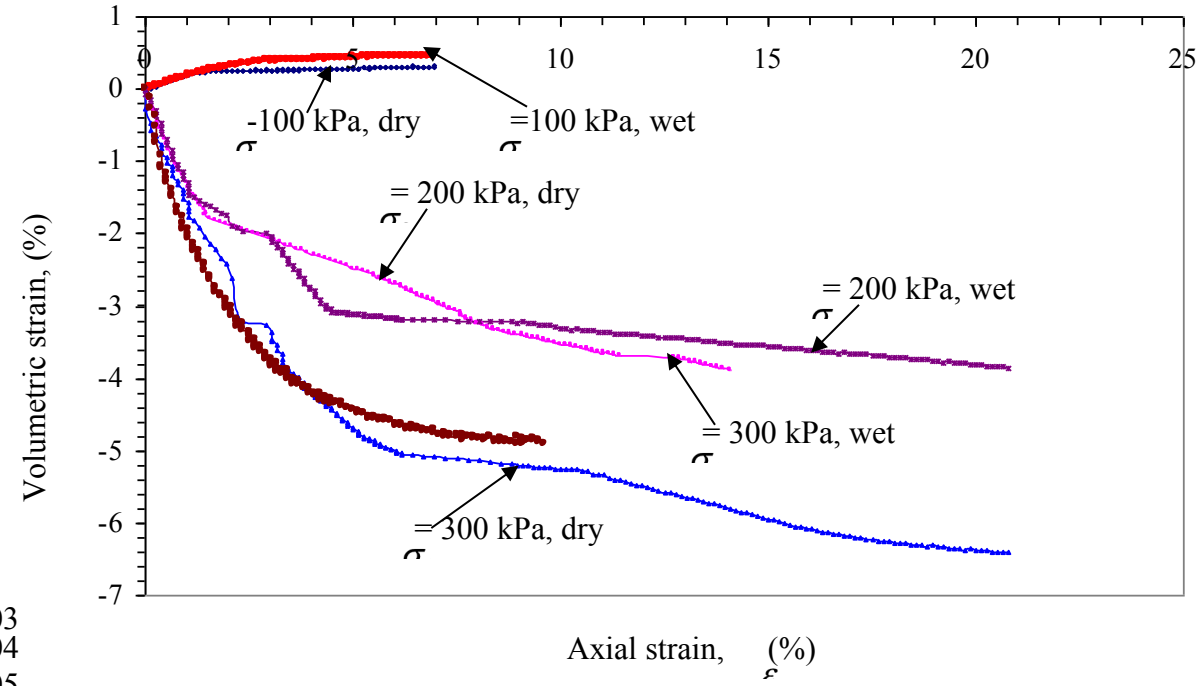

803
804
805
806

(b)

807
808
809

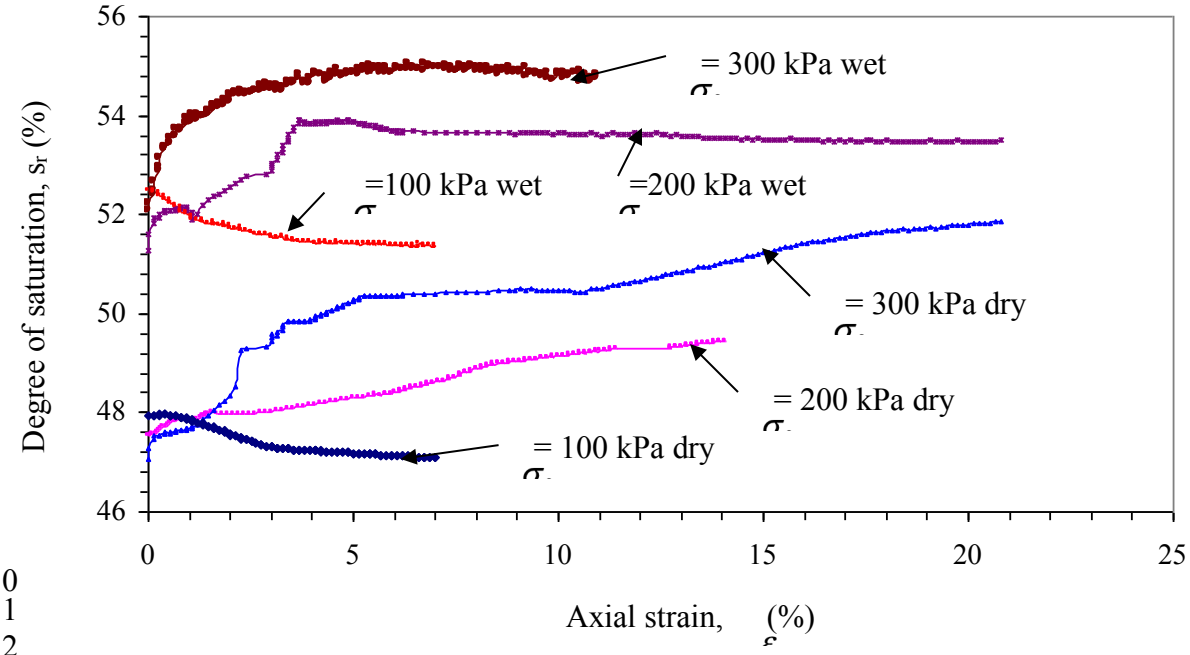

(c)

Fig.6. Results for drained tests on samples with *s* =200 kPa, under different cell pressures on the dry and wet sides: (a) deviator stress vs axial strain; (b) volumetric strain vs axial strain; (c) degree of saturation vs axial strain

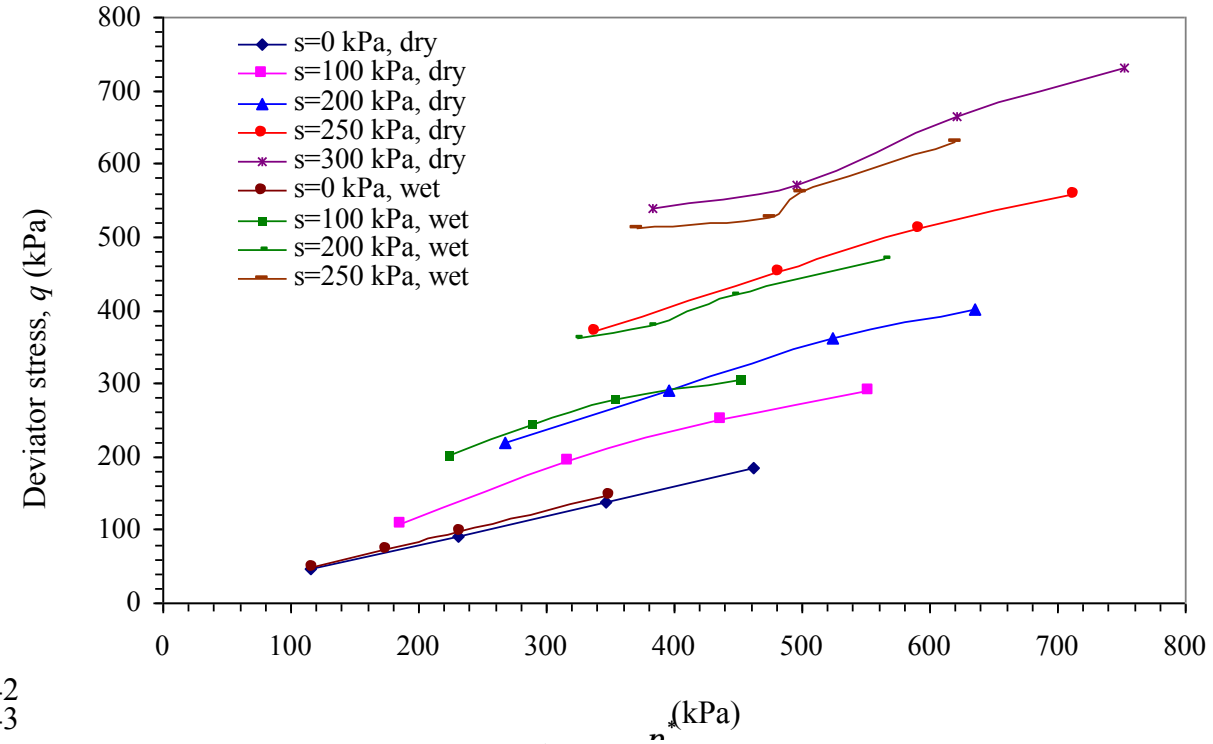

Fig.7. Critical state lines for q and p^* at various suctions for the drying and wetting paths

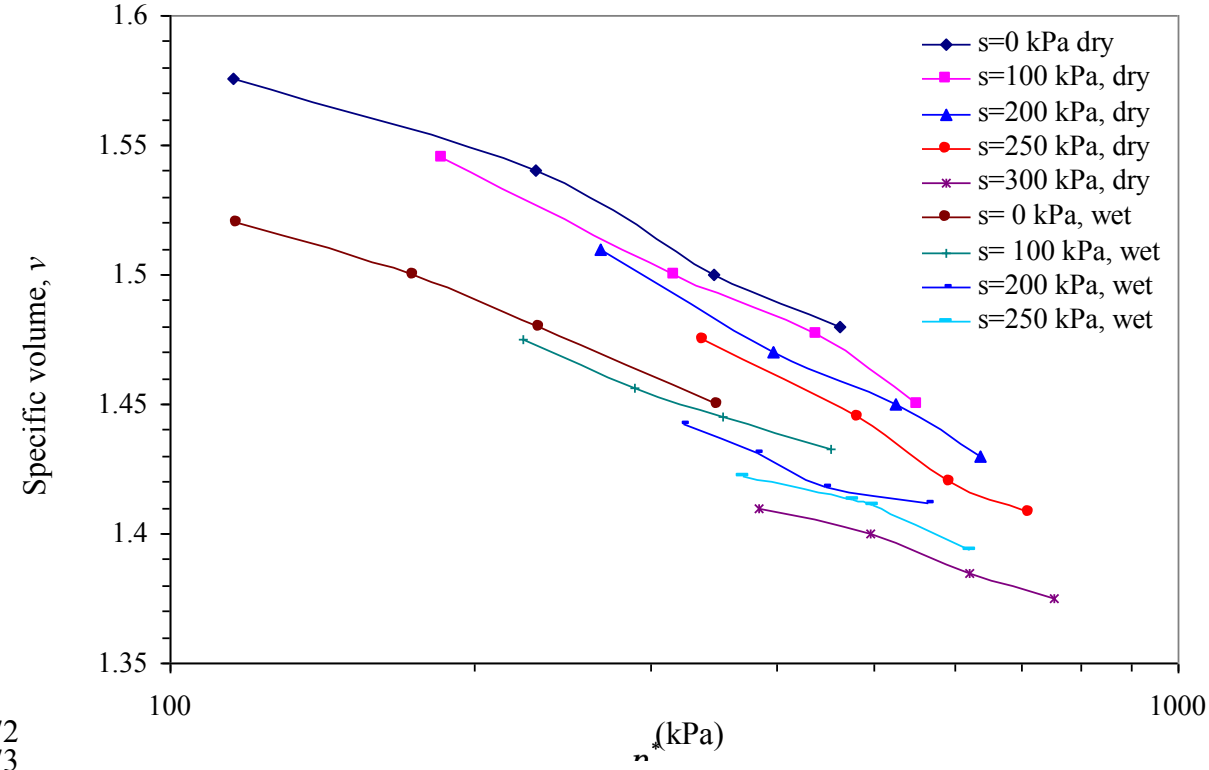

Fig.8. Variation of specific volume (v) and mean net stress (p^*) at critical state for the drying and wetting paths